Journal of Materials Chemistry A

Accepted Manuscript

ROYAL SOCIETY OF CHEMISTRY

www.rsc.org/materialsA

Journal of Materials Chemistry A

ARTICLE

Compressible Porous Hybrid Monoliths: Preparation via A Low-molecular Mass Gelators-based Gel Emulsion Approach and Exceptional Performances

Received 00th January 20xx,
Accepted 00th January 20xx

DOI: 10.1039/x0xx00000x

www.rsc.org/

Xiangli Chen, Lingling Liu, Kaiqiang Liu, Qing Miao, Yanchao Lü, Yu Fang*

A cholesteryl derivative, **BuDphe**, which is a low-molecular mass gelator (LMMG), was synthesized and used as a stabilizer for creation of a number of water/oil gel- emulsions, of which the oil could be a mixture of butyl methacrylate (*t*-BMA) and *p*-divinylbenzene (DVB), a mixture of *t*-BMA, DVB and polydimethylsilane (PDMS), or that of *t*-BMA, DVB, PDMS and trimethoxymethylsilane (MTMS). Polymerization of them resulted in porous polymeric or hybrid monoliths, **M-1**, **M-2**, **M-3**, **M-4** and **M-5**, respectively, of which the first is a pure poly-*t*-BMA monolith, the second to the fourth are the ones containing increasing amount of PDMS, and the last is a hybrid of poly-*t*-BMA, PDMS and hydrolyzed MTMS. The hybrid monoliths, in particular **M-5**, as prepared possess not only hydrophobicity, porosity, and low-density, but also an unprecedented flexibility in dry state with a maximum shape recovery corresponding to 100% of the original thickness after more than 70% compression strain. Moreover, silylanization also improves the thermo-stability of the porous materials. Absorption test demonstrated that **M-5** is an excellent absorbent for a number of organic solvents and oils. The material after absorption can be re-generated and the liquids absorbed can be recovered by simple squeezing. Furthermore, the absorption-separation process with CH_2Cl_2 as an example solvent could be repeated at least 10 times with no significant reduction of its absorption capacity. Combination of the excellent flexibility, great absorptivity, easiness in preparation, and low-energy consumption in drying makes the hybrid monoliths, in particular **M-5**.

Introduction

With fast industrialization, clean up organic pollutants, in particular oil leakages, has attracted increasing attention during the last few decades. This is because the pollutants may cause irrecoverable damage to eco-systems via contamination of water and soil. However, treatment of the pollutants in an efficient and practical way is a burning challenge to scientists working in the field. Till now, the most efficient way to clean up the pollutants from water is separation via selective absorption. Therefore, a lot of effort has been put into creation of new absorbents.[1-7] In fact, absorbents from natural materials such as expanded perlite, zeolites and graphite, as well as activated carbon, sawdust have long been used as absorbents, but the performance of them is not as good as expected because of low oil loading density and low oil-water selectivity.[1, 8] It is of the reasons that people has tend their attention to synthetic porous materials, including silicas,[9] carbon nanotubes,[10] organic-inorganic hybrids,[11] functionalized polymers and resins,[12,13] etc. For example, Wu and co-workers[10] reported a sponge-like material, which is composed of self-assembled, interconnected carbon nanotubes (CNT). The sponge in densified state swell instantaneously upon contact with organic liquids. Zhou and coworkers[14] prepared porous polystyrene, and the materials as prepared exhibit idea oil-water separation and gas permeability properties. Guo and colleagues[15] prepared special xerogels from a dendrimer of poly-propylenimine and a block co-polymer that is sulfonated polystyrene-block-poly-(ethylene-ran-butylene)-block-polystyrene. The porous materials could be used as oil absorbents for the clean-up of oil spills, and show high oil absorption capacity, ideal absorption speed, and in addition, the materials are reusable.
The materials or the methods used for the preparation of them, however, suffered from some drawbacks such as complicated preparation processes, high costs for reagents and apparatus, and energy-consuming for drying, which may prevent their real-life uses. In fact, with exception of some porous carbon materials and one silylated nanocellulose sponge which are cost-expensive, [10,16] other porous polymeric

Key Laboratory of Applied Surface and Colloid Chemistry (Shaanxi Normal University), Ministry of Education, School of Chemistry and Chemical Engineering, Shaanxi Normal University, Xi'an 710119, P. R. China. Fax: 0086- 29-81530787; Tel: 0086-29-81530788; E-mail: yfang@snnu.edu.cn

† Electronic Supplementary Information (ESI) available: [Figure S1 ^{1}H NMR spectra of BuDphe, Figure S2 FTIR spectra of BuDphe, Figure S3 MS spectra of BuDphe, Figure S4 Gelation behaviors of BuDphe in various solvents, Figure S5 Phase behavior of BuDphe/*t*-BMA (2%, wt%) after 10 minutes standing, Figure S6 Phase behaviour of BuDphe /water /*t*-BMA (total volume is 1 mL) with different water contents: (a) 0%, (b) 20%, (c) 50%, (d) 80%, (e) 100% (v/v), Figure S7 TGA curves of M-1 (black line), M-4 (red line), M-5 (blue line) under oxygen flow, Figure S8 (a) Maximum absorption capacities of M-5 to some organic-solvent mixtures*; (b) Selectivity of the materials to the solvents* under test, results from GC-MS studies, Table S1 Theoretical values of the porosities of the porous materials, Table S2 Experimentally determined porosities of the porous polymeric materials, Video S1 The porous composite monolith is still flexible after treatment in liquid nitrogen, Video S2 Compression test on weight illustrating spring-back behavior, Video S3 Selective absorption of gasoline from water by using M-5, Video S4 The absorption–squeezing processes with M-5 as a sample absorbent]. See DOI: 10.1039/x0xx00000x

absorbents reported till now are almost all hard, brittle and flammable in dry state, which make them very inconvenient in real-life uses. Therefore, creation of porous polymeric materials with low density, high strength, good toughness, maximum service life and low cost still remains a significant challenge.

For the preparation of the porous materials, various template methods have been employed, but among them the colloidal template is almost the most widely adopted one.[17-20] In a typical preparation, a biphasic system is generated and then the continuous phase is polymerized. The colloidal entities serve to create porosity in the final polymeric materials and are removed after polymerization. The colloidal systems could be emulsions,[21] micro-emulsions,[22,23] solid particles,[18,24,25] breath figure droplets,[26,27] and gel emulsions,[28-30] and the pore sizes can range from a few nanometres to hundreds of micros. Among the colloidal templates, gel emulsions are more unique due to the fact that their internal structures could be easily adjusted by varying their composition.

Gel emulsions were discovered earlier but only till 1966 a clear definition was given by Lissant and co-workers.[31] In the definition, gel-emulsions are recognized as two-phase systems, of which one is the continuous phase and the other the dispersed phase. In particular, the volume fraction of the second one is greater than 0.74, which is a critical value in geometry for a container to be fully filled by non-deformed balls. In other words, the continuous phase must be networked thin films with porous structures, which are the bases for them to be used as templates.[32-34] Accordingly, gel emulsion is also named as high internal phase emulsion (HIPE) and the porous polymeric monoliths obtained from them are named as "polyHIPE".[35]

It is not difficult to understand that the structure and property of the porous materials created in the template way are determined by the structure and the chemical nature of the gel-emulsions, of which they are produced from. By this token, development of gel-emulsions with distinctive structure and property is the priority in the creation of porous polymeric monoliths with predetermined structure and property. Practically, surfactants and micro-/nano-particles are commonly used as stabilizers, which are the third, but may be most variable component of gel-emulsions with the exception of water and water immiscible liquid.[36-39] Even though surfactants are easily found, available and most commonly used stabilizers, yet they are not very efficient since a large amount, 5–50% (w/v) of the continuous phase, is required. As for gel emulsions stabilized by micro-/nano-particles, the so called Pickering emulsions, they may suffer from phase inversion when the volume fraction of the dispersed phase reaches 0.65–0.70. Unlike these gel emulsions, a new kind of gel emulsions was reported by us recently, of which low-molecular mass gelators (LMMGs) were used as stabilizers.[28-30,40,41] The most distinct difference between the two kinds of gel emulsions is that both the continuous phase and the dispersed phase are liquids, but for the ones reported by us, the continuous phase is gelled due to presence of the LMMGs. It is the difference that makes the volume fraction of the dispersed phase need not to be greater than 0.74 because it is physically trapped within the continuous phase. Moreover, preparation of gel-emulsions by using LMMGs as stabilizers is so simple that only agitation at room temperature is required, and procedures like heating, cooling, and addition of co-solvent are not at all necessary, and furthermore, 2.5% (w/v) or even less than that of the stabilizer is enough to produce a gel-emulsion with good stability. No doubt, these advantages must be beneficial for the practical production of gel-emulsions, and for their template application.[42-46]

Herein, we report on the preparation of some new LMMGs-based gel-emulsions, and their utilization in the template preparation of porous poly-*t*-BMA and relevant hybrid monoliths, which exhibit good mechanical property, ideal oil absorptivity, and excellent reusability. In addition, the preparation is easy, the energy consumption is low, and their internal structure is highly adjustable. This paper reports the details.

Experimental

Materials

Tertiary butyl methacrylate (*t*-BMA, 99%, Sigma-Aldrich), acrylonitrile (AN, 99%, Sigma-Aldrich), styrene (St, 99%, Sigma-Aldrich), methyl methacrylate (MMA, 99%, Sigma-Aldrich) and *p*-divinylbenzene (DVB, Aldrich) were purified before use by passing through a neutral aluminum oxide column to eliminate the pre-added inhibitor in the reactants. After purification, the monomer and the cross-linker were stored in a freezer if they were not used directly. 2,2'-Azobis(isobutyronitrile) (AIBN, 97%) was purchased from Sigma-Aldrich, and was purified by recrystallization using ethanol before use. Sylgard 184 silicone elastomer base and curing agent were purchased from Dow Corning (Midland, USA), and Boc-phenylalanine was purchased from Chengdu enlai biological technology Co., LTD. Water used throughout was doubly distilled. Other reagents were of, at least, analytical grade, and used without further purification.

Syntheses of the cholesteryl derivative (BuDphe)

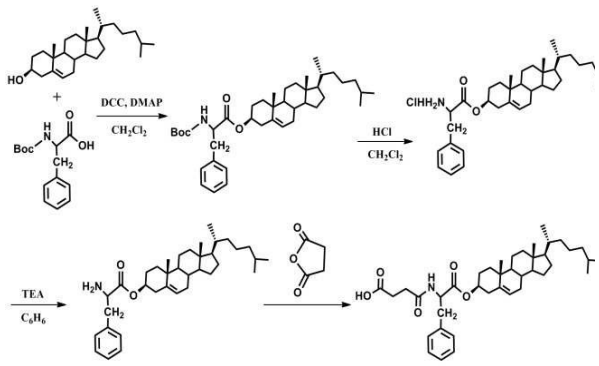

Scheme 1 The synthesis route of **BuDphe**

The methods used for the preparation of **BuDphe**, which is a succinic acid derivative of cholesteryl D-phenylalanine, are schematically shown in Scheme 1. Specifically, cholesteryl L-phenylalanine with a primary amine group in its end was synthesized according to a previous report.[47] The compound (5.34 g, 0.01 mol) was dissolved in 100 mL THF and stirred at room temperature to make sure its full dissolution. To the system, 100 mL THF solution of succinic anhydride (1.00 g, 0.01 mol) was added drop-wise. After the addition, the mixture was

heated and refluxed for 24 h. The reaction was monitored by TLC. Then, the mixture was filtered, and the filtrate was evaporated to dryness. The solid as obtained was re-crystallized from methanol for two times, and then dried in vacuum to give a desired product (**BuDphe**) in 70% yield as white powders. ^{1}H NMR ($CDCl_3$/Me_4Si， 400 MHz, Figure S1) : δ (ppm) 5.37 (t, alkenyl, 1H), 4.55-4.69 (m, CHCOO, 1H), 3.70-3.73 (m, oxycyclohexyl, 1H), 2.78-3.12 (m, $C_6H_5CH_2$, 2H), 0.68-1.99 (m, cholesteryl protons, 41H). FTIR (Figure S2): 3337 (NH), 2944 (CH), 1730 (C=O.-O), 1540 (NH, bending), 1209 (-C-O). HRMS (Figure S3): m/z calcd for [M - H^+]: 632.4393, found: 632.4331. Elemental analysis, Calc. for (found) $C_{42}H_{65}NO_5$: C 74.80 (75.79); H 9.27 (9.38); N 2.15 (2.21).

Gelation test

A weighted amount (0.025 g) of **BuDphe** and a measured volume (1 mL) of a chosen liquid were placed into a sealed test tube (diameter: 1.2 cm, height: 6 cm) and the mixture was oscillated at room temperature for 5 min, then the test tube was inversed to observe if a gel had been formed or not. Gels obtained after oscillation at room temperature were denoted as “G” (gel). In some cases, solution and solid-like gel may coexist within a system. This kind of system was referred to as “partial gel” (PG). For systems in which only solution was remained, they were denoted as “S” (solution). However, for systems in which the gelator could not be dissolved even at the boiling point of a liquid, they were defined as “I” (insoluble). Similar test was also conducted for mixture solvents of water and water immiscible organic liquids. At this case, gels were denoted as “GE”, and solutions “E”.

Gel-emulsion preparation

The gel emulsions used in the present studies could be prepared in the way as described below. For a typical system, its internal phase or dispersed phase is water, which accounts 80% of the total volume of the gel emulsion to be prepared, and the remaining is the continuous phase, which contains nearly 72% of monomer liquids (t-BMA, St or MMA), 25% of DVB, 2% of the gelator, **BuDphe**, and 1% of AIBN. To make a gel emulsion, a given amount of water was added, in a drop-wise manner, into the organic phase under stirring, and then the system (a homogeneous emulsion) becomes a gel after a while at room temperature. For the introduction of silanes, two different ways were adopted. One is dissolved into the continuous phase, the oil phase, directly, and the other is physically dispersed into the dispersed phase, water, since they are water insoluble.

Template preparation of porous polymeric monoliths

The gel emulsion as prepared was heated to 40 °C and maintained at the temperature for 4 h in an oil bath to start pre-polymerization, and then the temperature of the bath was raised to 85 °C and reacted at the temperature for another 12 h to complete the polymerization. After polymerization, the monolith was removed from the reaction vessel, and then washed with ethanol (50 mL) four times. Finally, the polymeric monolith was naturally dried at ambient temperature until its weight became constant.

Characterization of the gel-emulsion

SEM observation of xerogel

SEM images of the xerogel were taken on a Quanta 200 scanning electron microscope (Philips-FEI). The accelerating voltage was 20 kV and the emission current was 10.0 mA. The xerogel for the measurement was prepared by freezing the gel formed in the concerned liquid at a measured concentration in liquid nitrogen, and evaporated by a vacuum pump for 24 h. Before the examination, the sample was attached to a copper holder by conductive adhesive tape, and then it was coated with a thin layer of gold.

Characterization of the monoliths

SEM observation

The diameters of the pores and pore throats of the porous polymeric or hybrid monoliths as prepared were semi-quantitatively calculated by using the images taken on a Quanta 200 Scanning Electron Microscopy spectrometer (Philips-FEI, 15 kV and 10 mA). Prior to observation, approximately 1 cm^3 of each sample was mounted on a sample holder and sputtered with gold for 80 s to ensure sufficient conductivity. The pore size was also measured through the SEM images using software of Image J. The pore sizes of the porous materials as created were measured in a literature method, that is for each measurement, more than 100 pores were taken into account.[48]

TGA measurements

Thermo-gravimetric analysis (TGA) was conducted on a thermal analyser (Q1000 DSC+LNCS+FACS Q600SDT). All the measurements were run at a heating rate of 10℃/min from 15 to 800 ℃ in oxygen atmosphere.

Mechanical measurements

Mechanical testing under compression with a CTM 2500 universal testing machine frame, following the testing procedures specified in ASTM D1621-04a (Standard Test Method for Compressive Properties of Rigid Cellular Plastics). The length and diameter of the specimen used for the test are 2.0 cm and 1.0 cm, respectively.

Hydrophilic and lipophilic tests

The contact angle of the monolith was measured in a routine way on a Dataphysics OCA20 contact-angle system at ambient temperature.

Density and total porosity determination

The bulk density (ρ) was determined by cutting the samples to an cylindrical shape and subsequently measuring the diameter (d), thickness(h) and weight (m).

$$\rho = \frac{m}{\pi(\frac{d}{2})^2 h} \quad (1)$$

The total porosity was calculated using following equation.

$$\Phi = \frac{\frac{m_2 - m_1}{\rho_1}}{\pi(\frac{d}{2})^2 h} \quad (2)$$

Where Φ is the total porosity, m_2 is the weight of the wet monolith saturated with bromobenzene. The solvent was chosen because it is of high boiling point, high-density, and miscible with the porous materials but not swell, m_1 is the initial weight of the monolith, and ρ_1 the density of bromobenzene.

Oil sorption test

To analyse the absorption capacity of a monolith, the monolith with known weight was placed in a small glass beaker filled with 10 mL of a neat organic liquid under test. After a certain time of absorption, the wet monolith was drained for 1 min until no residual droplet left on the surface. Each test was conducted for at least three times. The absorption capacity was then calculated via the following equation.

$$q = (m_s - m_0)/m_0 \quad (3)$$

Where q is the absorption capacity (g/g), m_s is the weight of the wet monolith after 5 min of drainage (g), and m_o is the initial weight of the monolith (g). As for absorption capacity represented in a way of g/cm^3, the value can be calculated by times of the q with ρ, the density of the corresponding absorbent.

Reusability test of the monoliths

To test the reusability, a wet monolith was centrifuged as hard as possible to get rid of the oil absorbed. The monolith was then washed completely with alcohol or some other suitable volatile organic solvent, followed by simple air-drying. Finally, the regenerated porous monolith was reused for the selective absorption of oil from water. This absorption and regeneration process was repeated for several times with gasoline-water as an example of oil-water mixture system.

Absorption selectivity test

The absorption selectivity of **M-5** to different organic solvents was conducted in a way similar to that used for oil sorption test. The only difference is organic solvent mixtures were used instead of the pure solvent. The compositions of the original mixtures and those obtained from the monolith were determined by GC-MS. The GC-MS measurements were performed on a Shimadzu GC-17A gas chromatograph coupled to a GCMS-QP 500 electron ionization mass spectrometer. During the entire course of the measurements, the sample remains under high purity helium. The chromatography was carried out by temperature programming at 5 °C /min rate, from 30 to 120 °C. The mass spectroscopy had a range of 50-200 atomic mass units. All samples before the measurements were diluted 100 times with toluene.

Results and Discussion

Gelation and gel emulsion formation

The gelation and gel emulsion formation properties of the compound, BuDphe, as produced were studied in a number of solvents and solvents/water mixtures, and the results are shown in Table 1 and Figure S4.

With reference to the table 1 and Figure S4, it is seen that BuDphe gels the alkyl solvents (*n*-heptane, *n*-octane, *n*-nonane, *n*-decane) but dissolves in tertiary butyl methacrylate (*t*-BMA), methyl methacrylate (MMA), and styrene (St) at room temperature. However, for the system of *t*-BMA, a partial gel was formed after 10 minutes standing (c.f. Figure S5). Interestingly, introduction of water into the alkyl solvents and *t*-BMA solution of BuDphe, and followed by vigorous shaking of the mixtures several minutes resulted in non-flowable emulsions, the so-called gel-emulsions. As described, the method used for the preparation of this gel-emulsion is simple and effective, and furthermore BuDphe is an efficient stabilizer due to the fact that 2% (*w/v*) of it is enough to create a gel-emulsion with good stability as evidenced by the observation that there is no seepage from the system after a month-long storage in a sealed bottle. Unlike the preparation of conventional gel-emulsions where surfactants or micro-/nano-particles are used as stabilizers, our method is straightforward that only agitation under room temperature is needed, thus heating, cooling, and addition of co-solvents are not at all required. No doubt the simpleness in preparation will definitely benefit practical uses when the process needs to be amplified. It is also worthy well to mention that the volume fraction of the dispersed phase could be as high as 95% (*v/v*).

Table 1 Gelation behaviors of **BuDphe** in various solvents

Solvents	**BuDphe**	Mixture solvents (*v/v*)	**BuDphe**
n-hexane	G	*n*-hexane : H_2O = 2:8	GE
n-heptane	G	*n*-heptane : H_2O = 2:8	GE
n-octane	G	*n*-octane : H_2O = 2:8	GE
n-nonane	G	*n*-nonane : H_2O = 2:8	GE
n-decane	G	*n*-decane : H_2O = 2:8	GE
t-BMA	PG	*t*-BMA : H_2O = 2:8	GE
MMA	S	MMA : H_2O = 2:8	E
St	S	St : H2O = 2:8	E

S = solution, I = insoluble, G = gel, PG = partial gel, GE = gel-emulsion, E = emulsion

To evaluate the effect of water content on the phase behaviour of the gel-emulsions, BuDphe /water /*t*-BMA was adopted as an example system, and the results are shown in Figure S6. Reference to the figures reveals that 2% (*w/v*) of BuDphe dissolves in *t*-BMA with no difficult (Figure S6a). However, introduction of water into the solution resulted in gelation as demonstrated in the pictures shown in Figures S6b, S6c and S6d. For pure water, the compound will stay in solid state, and no obvious change occurs in the liquid phase (Figure S6e), suggesting that BuDphe is insoluble in water.

Considering the fact that the volume fraction of water in the gel-emulsions as produced can vary from 20% to 95%, of which the value of 20% is significantly lower than the critical value of 74%, which is the lowest value for conventional gel emulsions.

It should be no doubt that this extension must be beneficial to the template preparation of low-density materials since the controllable range of the internal structure and density of the materials is broadened.

To know the details of the microstructures of the gel-emulsions, the systems of BuDphe/water/*t*-BMA with three different water contents of 20%, 50% and 80%, of which the gelator content is always 2% (w/v) of the continuous phase, were employed for SEM studies. The xerogels from them were meticulously prepared in a way described in the experimental section. Figure 1 shows some of the results. With reference to the images, it can be seen that the internal structures of the xerogels change along with water contents. Specifically, the porosity of the xerogels increases along with increasing water content (c.f. Figure 1), which is not difficult to understand because more water means less volume fraction of the continuous phase and less BuDphe, and accordingly greater porosity of the gelator aggregates.

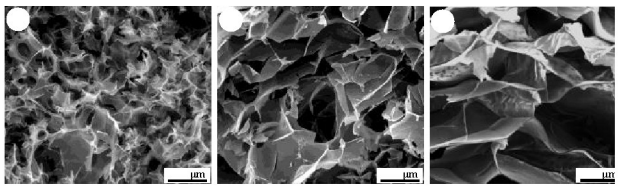

Figure 1 SEM images of the xerogels prepared from different gel-emulsions of **BuDphe**/water/ *t*-BMA (total volume, 1 mL) of different water contents: (a) 20%, (b) 50%, (c) 80%.

Template application

For preparation of porous polymeric materials, polymerization of the continuous phase of a gel emulsion is a commonly adopted strategy (c.f. Figure 2a). For the present study, free radical polymerization was chosen, of which the monomer, the cross-linker and the initiator in the phase adopted are *t*-BMA, DVB and AIBN, respectively. After optimization of the parameters, a stable gel emulsion was obtained, of which the recipe is listed in Table 2.

Table 2 A typical recipe of a stable gel emulsion

	Components	Amounts
Organic phase continuous phase	Monomer	15% of the total volume (*v/v*)
	Stabilizer	2% of the monomer (*w/v*)
	Cross-linker	1/3 of the monomer (*v/v*)
	Initiator	1% of the monomer (*w/v*)
Aqueous phase dispersed phase	Water	80% of the total volume (*v/v*)

With the recipe, a porous poly-*t*-BMA monolith (**M-1**) was obtained. The porosity of the monolith was confirmed by SEM studies (c.f. Figure 2b). It is seen that the pores, which are the remains of the water droplets of the dispersed phase, possess limited throats, in other words, they are relatively isolated from each other. Quantitative measurements revealed that the average diameter of the pores is around 55 μm, the bulk crush strength 0.9 MPa, and the density 0.18 g/cm^3. As for the porosity of the materials, it is hard to be measured by a routine method, such as BET and mercury intrusion due to pore size or miscibility problem. To have a semi-quantitative understanding of the porous structures of the materials, a theoretical porosity can be calculated by considering the bulky density of the material and the density of polymeric material itself (c.f. Table S1 and the relevant information). In fact the parameter of the materials can be also measured experimentally in a way similar to that of mercury intrusion method by choosing a suitable organic liquid (c.f. equation 2). The results from the calculation and the test are 0.80 and 0.89, respectively, as shown in Tables S1, S2.

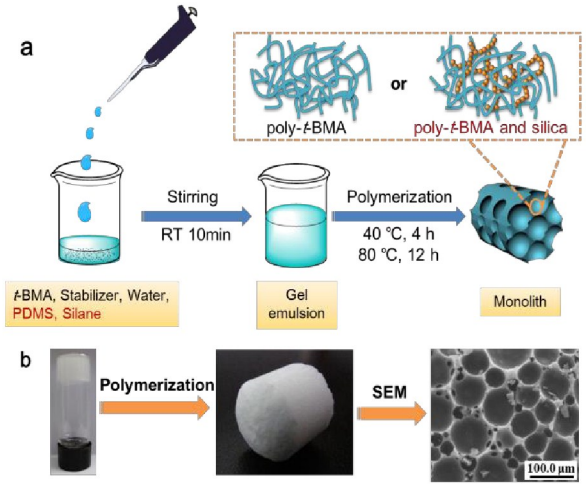

Figure 2 a) Illustration of the procedures adopted for the preparation of the porous polymeric monoliths, b) Photos and SEM image of the gel-emulsion, the porous poly-*t*-BMA monolith and the internal structure of the material.

Modification of the porous polymeric monoliths

Mechanically, **M-1** is very fragile, and this weakness must impede its application. Therefore, it is necessary to find a way to improve the mechanical property of the materials. It is lucky to find that introduction of PDMS, which is inert, non-toxic, non-flammable and acts as viscous liquid at high temperature but rubber-like solid at low temperature, into the continuous phase before polymerization does not affect the phase behaviour of the gel emulsion, and thereby porous hybrid monoliths can be obtained via simple polymerization of the PDMS containing systems. In this way, four monoliths, which are **M-1**, **M-2**, **M-3**, and **M-4**, respectively, with different compositions were produced, of which PDMS contents of the initial reaction systems are 0%, 2%, 5%, and 10% (w/v), respectively.

Table 3 Elasticity of $\sigma_{50\%}$, crush strengths, apparent densities, and theoretical porosities of the porous composite monoliths produced via a gel emulsion template approach and their parent porous polymeric monolith.

Porous Monoliths	Elasticity of $\sigma_{50\%}$	Crush strength (MPa)	Apparent density (g/cm^3)	Porosities	
				Φ_t	Φ
M-1		0.9	0.18	0.80	0.89
M-2	2.1	3.4	0.21	0.77	0.90
M-3	1.3	5.6	0.24	0.74	0.87
M-4	0.9	~	0.25	0.73	0.89
M-5	1.3	~	0.27	0.71	0.84

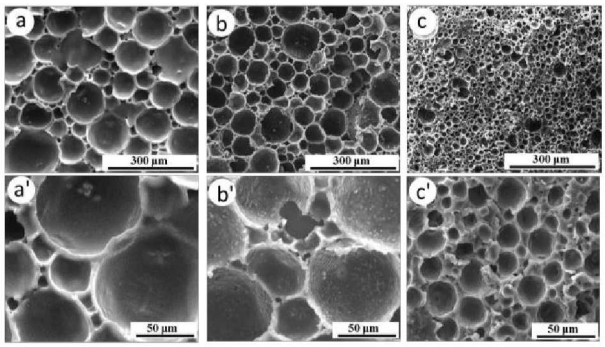

Figure 3 SEM images of the internal structures of the monoliths with three typical PDMS contents of (2, 5, 10, *wt*%)

To interrogate the internal structure difference of the porous hybrid materials as obtained, SEM measurements of the materials were performed, and the results are shown in Figure 3. It is clearly seen that with increasing PDMS content in the reaction systems, the porosity of the monolith decreased, but the density increased from 0.18 to 0.25 g/cm^3. (c.f. Table 3) The correlation between the monolith structure and the gel-emulsion composition demonstrates the extraordinary adjustability of the internal structures and densities of the porous materials. It is believed that incorporation of PDMS must bring the final materials some extraordinary properties such as toughness, as evidenced by greatly improved flexibility. Stress-strain curve is an extremely important graphical measure of a material's mechanical property, and thereby compression tests were conducted to understand the tune-ability of the mechanical properties of the porous materials via incorporation of PDMS into the porous poly-*t*-BMA scaffold.

Inspection of Figure 4a, it is seen that M-1 exhibits linear stress-strain behaviour below 7% strain, which might be a result of the elastic deformation of the monolith at low strains. However, further increase the strain, the stress-strain curve deviates from the linearity, of which the reason behind might be a progressive collapse of the polymer scaffold. It is to be noted that the scaffold is collapsed when the strain reaches ~48%. The substantial plastic deformation as noted from the figure on unloading can be assigned to the irreversible collapse of the sample during compression.[8] It is interesting to note that further increase the content of PDMS in the hybrid porous

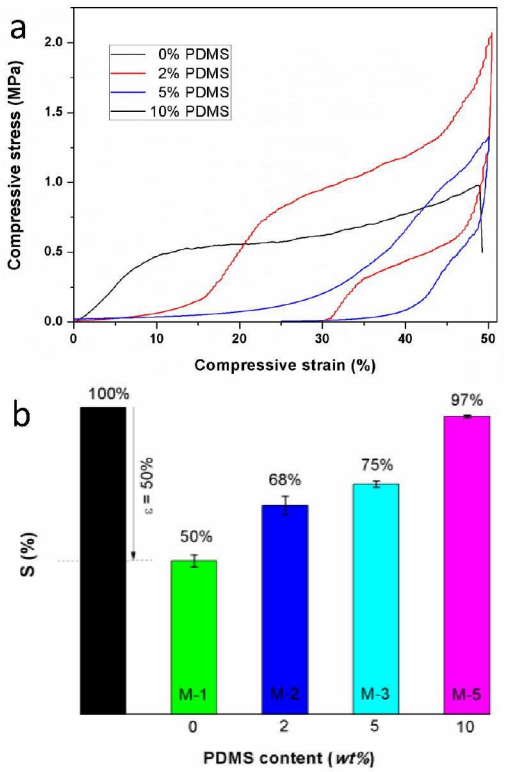

Figure 4 (a) Compressive stress-strain curves of the monoliths with four different PDMS contents of 0, 2, 5, and 10wt%, respectively, of which the data were obtained before 50% compression strain. (b) Thickness recovery (*S*) of the monoliths upon unloading from a compressed state (ε = 50%). The relative thickness of the monoliths after unloading is visualized by columns.

monoliths resulted in more flexible materials as evidenced by the fact that they are not crushable at least within a 50% strain. Further inspection of the curves, it also can be seen that with increasing PDMS contents in the hybrid monoliths from 2%, 5% to 10% (w/v), the flexibility of the materials increases as the stress at 50% deformation ($\sigma_{50\%}$) decreased from 2.1 MPa, 1.3 MPa to 0.9 MPa. Furthermore, the strains corresponding to the crush of the materials increased from 0.9 to 3.4, and then

to 5.6 along with increasing the PDMS contents (c.f. Table 3). Unlike other polymers, PDMS is typical because it has a glass transition temperature of less than -120 °C that means it is in the rubber state at room temperature. Clearly, it is the contribution of PDMS that makes the hybrid monoliths possesses increased flexibility.

The shape recovery of the PDMS containing monoliths was evaluated by recording the residual strains (ε_{final}) after unloading the compressed specimens. The height recovery *S*, expressed as the percentage of the original height, is plotted as a function of PDMS content in a histogram, which visually demonstrates the dependence of the value of *S* upon the PDMS content (Figure 4b). The unmodified monolith was crushed, and shows no any sign of recovery. For other specimens, the recovery percentage increases significantly with increasing PDMS content. Actually, for **M-4**, the recovery could be nearly 100% of its original height. To our knowledge, this is the first example of poly-HIPEs that shows such good flexibility. As for the decrease in the hardness of the porous materials, it could be attributed to the decrease in cross-linking density of poly-*t*-BMA scaffold due to presence of PDMS.[3,49]

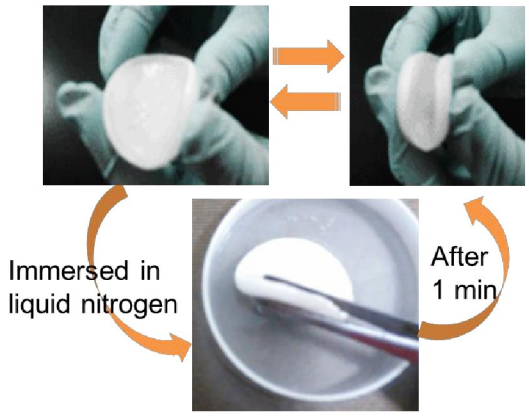

Figure 5 Photograph of flexibility (room temperature and immersed in liquid nitrogen)

Considering the change in the composition and in the structure of the materials, as well as the importance of thermo-stability for real-life uses, it should be worthy to evaluate the thermo-stability of the materials. Accordingly, thermo-gravimetric analysis (TGA) of the unmodified poly-*t*-BMAs (**M-1**) and one of the modified poly-*t*-BMAs (**M-4**) was conducted under oxygen atmosphere, and the results are shown in Figure S7. With reference to the traces, it is revealed that the thermo-stability of the PDMS modified material is slightly improved if compared to that of the unmodified one, even though full decomposition of the hybrid material is much more difficult as indicated by the fact that about 20% of **M-4** is still remained at 800 ºC. This result demonstrates that PDMS modification did not bring significant effect upon the thermo-stability of the original material, suggesting further research remains to be conducted. Furthermore, long time liquid nitrogen treatment did not show any significant effect to the flexibility of **M-4** as demonstrated by pictures shown in Figure 5 and a film shown in Video S1, a property crucial for them to find applications in extremely harsh environment such as polar zones.

Silane effect

To further improve the property of the porous monoliths, trimethoxymethylsilane (MTMS) was used instead of 90% of *t*-BMA (v/v). Fortunately, the system was still remained as a gel-emulsion, and polymerization resulted in a sponge-like hybrid monolith (**M-5**), which shows excellent mechanical properties as will be described below. The TGA result of this specimen was also shown in Figure S7. It is seen that the thermo-stability of **M-5** is superior to those of **M-1** and **M-4**, and its significant decomposition starts much beyond 300 C, indicating that **M-5** possesses good ablation resistance. Moreover, **M-5** shows little permanent compression set, and almost no change in mechanical response over 25 compression cycles for a strain up to 50% (Figures. 6a, 6b). The Young's modulus of the monolith is about 2.6 MPa, significantly lower than the values (10^1 to 10^3 MPa) for porous materials from inorganic or glassy particles.[51] This result suggests that structurally M-5 may have some similarities to the porous materials from inorganic or glassy particles even though it contains organic components, which in turn explains why the Young's modulus of M-5 is lower than its count part, the pure inorganic porous materials. This argument is supported by the results from SEM and corresponding element mapping studies as shown in Figure 7.

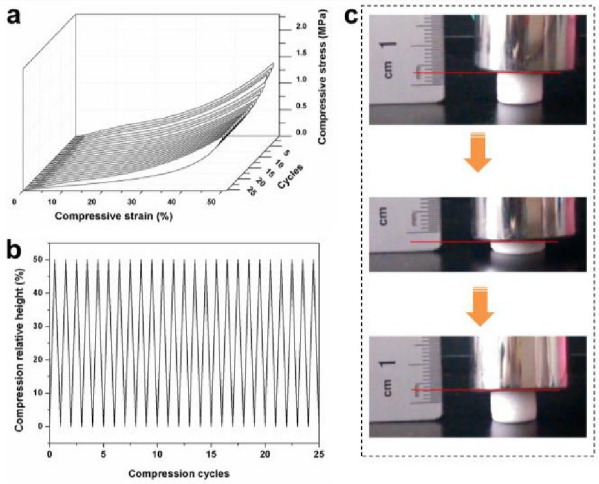

Figure 6 a) Compressive stress-strain curves of the monolith of **M-5** compressed to 50% strain, b) **M-5** along the compression axis during cyclic compression to 50% of its original size (Note: the compression was repeated for 25 times, and the scaffold regains its original size after each compression, and c) Sequential photographs of compression test illustrating spring-back behaviour.

References to the SEM images (Figures 7a, 7b) and the element mappings (Figures 7c, 7d), it is clearly seen that the silica particles resulted from decomposition of MTMS deposited in the polymeric materials, at least on the surfaces of the void walls. It is the special soft (organic polymer)-hard (inorganic silica) hybrid structure that may allow the silica particles to slide within a certain range, and create several conformational states. Recovery happens possibly due to entropic response to the deformations.[49,50] Further tests

Table 4 Comparison of adsorption capacities of absorbents

Absorbents	Components	Adsorption solvents	Adsorption capacity (g/g)	Reference
Polystyrene HIPE	CMs/Styrene/DVB/ Span80	toluene	29.5	[14]
Poly hybrid HIPE	SSEBS/ PPI dendrimers	chloroform gasoline crude oil	32.2 21.2 15.1	[15]
Polystyrene HIPE	**CDDE**/ Styrene/DVB	dichloromethane gasoline	20.29 16.49	[28]
Poly-*t*-BMA HIPE	Compound **1**/ *t*-BMA/DVB/ 3-isocyanatopropyltriethoxysilane	dichloromethane kerosene	17.33 8.17	[29]
Poly hybrid HIPE	SSEBS/–NH_2 modified Fe_3O_4 nanoparticles	xylene gasoline	26 21	[51]
Polystyrene HIPE	Allyl-β-CD/ styrene/DVB / Span80	phenol *p*-chlorophenol 2,4,6-trichloro-phenol	5.74 6.93 8.16	[52]
Poly hybrid HIPE	**BuDphe**/ *t*-BMA/DVB/PDMS/ MTMS	dichloromethane benzene *n*-hexane gasoline	35.7 (± 0.83) 30.2 (± 0.93) 20.0 (± 1.13) 16.1 (± 1.12)	This work

(Figure 6c, Video S2) demonstrated that the porous hybrid monolith of M-5 regains its original height after more than 70% compression strain, an unprecedented property reported in literatures for porous inorganic-organic hybrid materials prepared by using a HIPE-based template method.

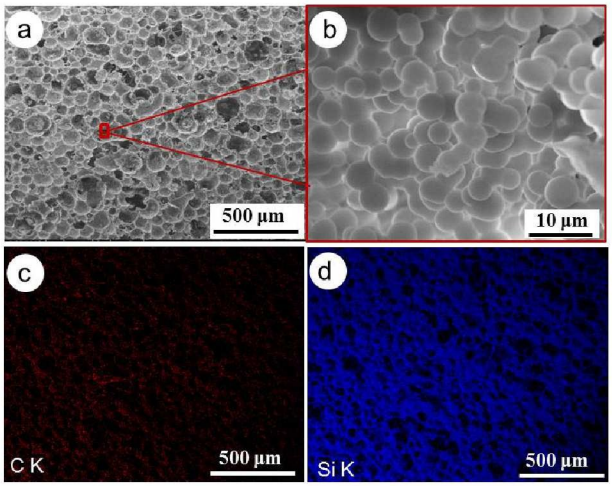

Figure 7 SEM image of the MTMS modified porous polymeric monolith (**M-5**, a), SEM image of its internal structures with larger magnification times (b), C and Si EDX element mappings of **M-5** (c, d).

Oil absorption

Owing to structure, hydrophobicity and mechanical stability, the porous hybrid **M-5** might be an ideal absorbent of some organic pollutants and oils. As shown in video S3, when a small piece of **M-5** (a thinly sliced sample) was put into contact with gasoline, it absorbed the oil completely within a few seconds, resulting in clean water which was originally contaminated by the oil. Interestingly, **M-5** is always floating on the water surface even after saturated with gasoline, and this must bring convenience for subsequent separation.

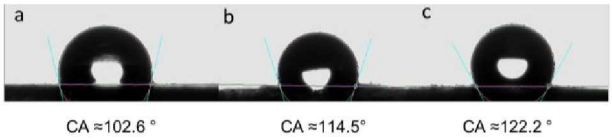

Figure 8 Images of contact angles with water of three porous materials, where a, b, and c are the images of the materials of **M-1**, **M-4** and **M-5**, respectively.

To have a quantitative understanding of the absorption capacity, a concept of absorption efficiency was introduced, and it is defined as weight gain, wt%, which is the weight of absorbed substance per unit weight of the pristine M-5. In this way, a number of commonly used organic solvents and oils such as hydrocarbons (n-hexane and cyclohexene), aromatics (toluene and benzene), and commercial petroleum products (gasoline, kerosene), as well as CH_2Cl_2 and THF, which are also commonly found in pollutants, were adopted as samples to test the absorption capacity of M-5, and the results are displayed in Figure 9a. It is seen that M-5 absorbs the liquids, in average, up to 10.6(± 1.21) to 35.7(± 0.83) times of its own weight, a result comparable to the best results reported in the literatures (c.f. Table 4). The superior performances of the materials created in the present study may be understood by considering its unique internal structures and compositions. As it is well-known that the absorption capacity of a porous monolith to organic solvents must be determined by many factors, including but not limited to the porosity, the internal structures, the chemical nature, and even the swelling ability

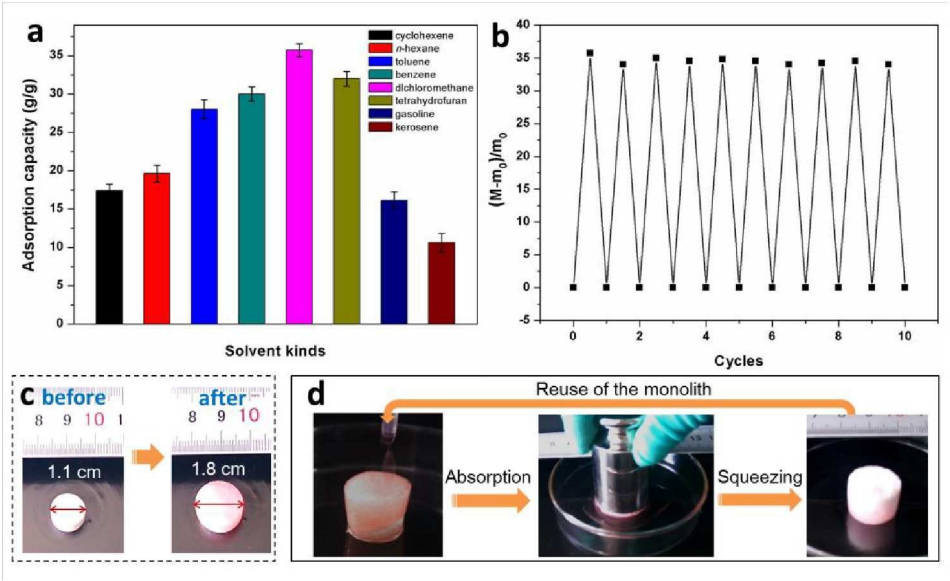

Figure 9 a) Maximum oil adsorption capacities of **M-5** to eight different organic liquids*, b) CH_2Cl_2 adsorption and reusability of the monolith, c) Photos of **M-5** before and after gasoline adsorption, and d) Snapshots of the process of the adsorption squeezing cycles.

* Quantification test demonstrated that leaching of the liquid absorbed is negligible (c.f. Table S3 and relevant text in the Supporting Information).

of the materials, which is a property well related with the crosslinking density of the materials. For our monolith, it is not only highly porous and hydrophobic as shown in Figure 7 and Figure 8, but also it is swell-able, a property rarely found in other porous materials prepared via a gel-emulsion technique.

The sorption test was further conducted with organic solvent mixtures as samples. The results are shown in Figure S8. The relevant discussions are also provided (c.f. page S10-S12, Supporting Information).

From a viewpoint of practical uses, the recyclability of an absorbent is another crucial criterion to judge whether it is practically applicable. Therefore, the usability of **M-5** was studied with CH_2Cl_2 as a sample liquid. During the test, the solvent absorbed was squeezed out mainly thanks to its flexibility (c.f. Video 4). The absorbent as recovered was washed several times with volatile and less toxic organic solvents, such as ethanol, and then naturally dried. The test was repeated for 10 times, and the results are depicted in Figure 9b. It is clearly seen that both the absorption and the recovery are fully reversible, indicating a very bright future for real-life uses. Compared with other oil-removing materials reported in the literatures, the superiorities of the materials created in the present study included not only their high efficiency, reusability, low-energy consumption, environmental benign, but also their flexibility in dry state, which is crucial for their transportation and storage, a key issue in real-life application.

Conclusions

A cholesteryl derivative, **BuDphe**, which is a typical LMMG, was synthesized and successfully used as a stabilizer for the creation of water in *t*-BMA gel-emulsion. Polymerization of the continuous phase, *t*-BMA, resulted in porous poly-*t*-BMA monolith with controllable internal structure and density. To improve the mechanical properties of the materials, PDMS and a silane were employed as modifiers to prepare porous hybrid polymeric monoliths. As expected, the hybrid monoliths as prepared possess not only hydrophobicity, porosity, and low-density, which are the characteristics of the pristine poly-*t*-BMA monolith, but also flexibility in dry state, which is a property rarely found for other porosity polymeric monoliths prepared in a gel-emulsion template method and is crucial for real-life uses due to its convenience in transportation and storage. Moreover, modification, in particular when silanes were used as modifiers, also improves the thermo-stability of porous materials. Absorption test demonstrated that the silane modified porous monolith (**M-5**) can be used as an excellent absorbent for a number of commonly found organic solvents or oils. The materials after absorption are easy to be re-generated and the liquids absorbed can be collected by simple squeezing. Re-usability test with CH_2Cl_2 as an example solvent demonstrated that the monolith of **M-5** could be recycled for at least 10 times with no significant reduction of its absorption capability. Therefore, it is believed that the gel-emulsion template method developed for the preparation of the porous hybrid monoliths is versatile and facile, and shows bright future for synthesizing advanced, in particular, porous low density materials with superior oil-water separation properties.

Acknowledgements

This work was supported by the Natural Science Foundation of China (21473110 and 21273141), the 111 project (B14041), the

Program for Changjiang Scholars and Innovative Research Team in University (IRT1070).

Notes and references

1 Silverstein, M. S. Prog. Polym. Sci. 2014, 39, 199.
2 Wu, D.; Xu, F.; Sun, B.; Fu, R.; He, H.; Matyjaszewski, K. Chem. Rev. 2012, 112, 3959.
3 Xing, Y.; Deng, W.; Wang, H.; Gong, C.; Zhang, X.; Jie, J. J. Nanosci. Nanotechno. 2015, 15, 4450.
4 M. Kubín, P. Š. a. R. C. Collect. Czech. Chem. Commun. 1967, 32, 3881.
5 Peng, J.; Liu, Q.; Xu, Z.; Masliyah, J. Adv. Funct. Mater. 2012, 22, 1732.
6 Alagha, L.; Wang, S.; Xu, Z.; Masliyah, J. J. Phys. Chem. C 2011, 115, 15390.
7 Long, J.; Li, H.; Xu, Z.; Masliyah, J. H. Energ. Fuel. 2011, 25, 701.
8 Zhu, Q.; Pan, Q.; Liu, F. J. Phys. Chem. C 2011, 115, 17464.
9 Sayari, A.; Hamoudi, S.; Yang, Y. Chem. Mater. 2005, 17, 212.
10 Gui, X.; Wei, J.; Wang, K.; Cao, A.; Zhu, H.; Jia, Y.; Shu, Q.; Wu, D. Adv. Mater. 2010, 22, 617.
11 Zhao, H.; Nagy, K. L. J. Colloid Interface Sci. 2004, 274, 613.
12 Janout, V.; Myers, S. B.; Register, R. A.; Regen, S. L. J. Am. Chem. Soc. 2007, 129, 5756.
13 Ono, T.; Sugimoto, T.; Shinkai, S.; Sada, K. Adv. Funct. Mater. 2008, 18, 3936.
14 Yu, S.; Tan, H.; Wang, J.; Liu, X.; Zhou, K. ACS Appl. Mater. Inter. 2015, 7, 6745.
15 Wu, Y.; Zhang, T.; Xu, Z.; Guo, Q. J. Mater. Chem. A 2015, 3, 1906.
16 Zhang, Z.; Sèbe, G.; Rentsch, D.; Zimmermann, T.; Tingaut, P. Chem. Mater. 2014, 26, 2659.
17 Bian, S.; Zheng, J.; Tang, X.; Yi, D.; Wang, Y.; Yang, W. Chem. Mater. 2015, 27, 1262.
18 Scholz, S.; Lercher, J. A. Chem. Mater. 2011, 23, 2091.
19 Fu, G.D.; Li, G. L.; Neoh, K. G.; Kang, E. T. Prog. Polym. Sci. 2011, 36, 127.
20 Zhang, X.; Blanchard, G. J. ACS Appl. Mater. Inter. 2015, 7, 6054.
21 Sugihara, Y.; Yamago, S.; Zetterlund, P. B. Macromolecules 2015, DOI: 10.1021/acs.macromol.5b00995.
22 Schmidt-Winkel, P.; Glinka, C. J.; Stucky, G. D. Langmuir 2000, 16, 356.
23 Ma, Y.; Liang, J.; Sun, H.; Wu, L.; Dang, Y.; Wu, Y. Chem. - Eur. J. 2012, 18, 526.
24 Binks, B. P. Adv. Mater. 2002, 14, 1824.
25 Binks, B. P.; Clint, J. H.; Whitby, C. P. Langmuir 2005, 21, 5307.
26 Boker, A.; Lin, Y.; Chiapperini, K.; Horowitz, R.; Thompson, M.; Carreon, V.; Xu, T.; Abetz, C.; Skaff, H.; Dinsmore, A. D.; Emrick, T.; Russell, T. P. Nat. Mater. 2004, 3, 302.
27 Stenzel, M. H.; Barner-Kowollik, C.; Davis, T. P. J. Polym. Sci., Part A: Polym. Chem. 2006, 44, 2363.
28 Chen, X.; Liu, L.; Liu, K.; Miao, Q.; Fang, Y. J. Mater. Chem. A 2014, 2, 10081.
29 Jing, P.; Fang, X.; Yan, J.; Guo, J.; Fang, Y. J. Mater. Chem. A 2013, 1, 10135.
30 Miao, Q.; Chen, X.; Liu, L.; Peng, J.; Fang, Y. Langmuir 2014, 30, 13680.
31 Lissant, K. J. J. Colloid Interface Sci. 1966, 22, 409.
32 Lissant, K. J.; Peace, B. W.; Wu, S. H.; Mayhan, K. G. J. Colloid Interface Sci. 1974, 47, 416.
33 Chen, Y.; Ballard, N.; Gayet, F.; Bon, S. A. F. Chem. Commun. 2012, 48, 1117.
34 He, H.; Li, W.; Lamson, M.; Zhong, M.; Konkolewicz, D.; Hui, C. M.; Yaccato, K.; Rappold, T.; Sugar, G.; David, N. E.; Damodaran, K.; Natesakhawat, S.; Nulwala, H.; Matyjaszewski, K. Polymer 2014, 55, 385.
35 Cameron, N. R. Polymer 2005, 46, 1439.
36 Esquena, J.; Nestor, J.; Vílchez, A.; Aramaki, K.; Solans, C. Langmuir 2012, 28, 12334.
37 Nikiforidis, C. V.; Scholten, E. Food Hydrocolloid. 2015, 43, 283.
38 Princen, H. M. J. Colloid Interface Sci. 1983, 91, 160.
39 Dunstan, T. S.; Fletcher, P. D. I.; Mashinchi, S. Langmuir 2011, 28, 339.
40 Chen, X.; Liu, K.; He, P.; Zhang, H.; Fang, Y. Langmuir 2012, 28, 9275.
41 Peng, J.; Xia, H.; Liu, K.; Gao, D.; Yang, M.; Yan, N.; Fang, Y. J. Colloid Interface Sci. 2009, 336, 780.
42 Mamak, M.; Coombs, N.; Ozin, G. Adv.Mater. 2000, 12, 198.
43 Leventis, N.; Sotiriou-Leventis, C.; Mohite, D. P.; Larimore, Z. J.; Mang, J. T.; Churu, G.; Lu, H. Chem. Mater. 2011, 23, 2250.
44 Sadekar, A. G.; Mahadik, S. S.; Bang, A. N.; Larimore, Z. J.; Wisner, C. A.; Bertino, M. F.; Kalkan, A. K.; Mang, J. T.; Sotiriou-Leventis, C.; Leventis, N. Chem. Mater. 2011, 24, 26.
45 Brun, N.; Babeau-Garcia, A.; Achard, M.-F.; Sanchez, C.; Durand, F.; Laurent, G.; Birot, M.; Deleuze, H.; Backov, R. Energ. Environ. Sci. 2011, 4, 2840.
46 Chen, X.; Wang, X.; Fu, X. Energ. Environ. Sci. 2009, 2, 872.
47 Li, Y.; Liu, K.; Liu, J.; Peng, J.; Feng, X.; Fang, Y. Langmuir 2006, 22, 7016.
48 Wang, J.; Zhang, C.; Du, Z.; Xiang, A.; Li, H. J. Colloid Interface Sci. 2008, 325, 453.
49 Rajamanickam, R.; Kumari, S.; Kumar, D.; Ghosh, S.; Kim, J. C.; Tae, G.; Sen Gupta, S.; Kumaraswamy, G. Chem. Mater. 2014, 26, 5161.
50 Luo, Y.; Wang, A.; Gao, X. Soft Matter 2012, 8, 1824.
51 Zhang, T.; Wu, Y.; Xu, Z.; Guo, Q. Chem. Commun. 2014, 50, 13821.
52 Han, J.; Xie, K.; Du, Z.; Zou, W.; Zhang, C. Carbohydr. Polym. 2015, 120, 85.